JOURNAL OF THERMOPHYSICS AND HEAT TRANSFER
Vol. 15, No. 3, July–September 2001

Thermophysical Properties of High-Thermal-Conductivity Graphite Sheets for Spacecraft Thermal Design

H. Nagano*
Keio University, Yokohama 223-8522, Japan
A. Ohnishi†
Institute of Space and Astronautical Science, Sagamihara 229-8510, Japan
and
Y. Nagasaka‡
Keio University, Yokohama 223-8522, Japan

Thermophysical properties of a new material—a graphite sheet, which has characteristics of high thermal conductivity, anisotropy, lightweight and flexibility—have been measured in order to apply this sheet to a spacecraft thermal control material. The following measurements were performed: 1) The thermal diffusivities in the in-plane and out-of-plane directions were measured over the temperature range from 100 to 350 K using a laser heating ac calorimetric method. 2) The specific heat and the total hemispherical emittance were measured over the temperature range from 173 to 375 K using a transient calorimetric method. 3) The solar absorptance was measured using a spectroscopic method for angles of incidence ranging from 5 to 60 deg. Additionally, the thermal conductivities and the specific thermal conductivities were calculated using the measured results, and the high potential of this graphite sheet as a material for spacecraft thermal control was confirmed.

Nomenclature

A	=	surface area, m^2
a	=	thermal diffusivity, $m^2\ s^{-1}$
a_{xy}, a_z	=	thermal diffusivity in respective direction, $m^2\ s^{-1}$
c	=	specific heat, $J\ kg^{-1}\ K^{-1}$
d	=	thickness of sample, m
f	=	modulating frequency, Hz
G_x, G_y, G_Z	=	Green's function for respective direction
J	=	spectral distribution of solar radiation, $W\ m^{-2}\ \mu m^{-1}$
k	=	wave number of temperature wave, m^{-1}
k_{xy}	=	wave number in the in-plane directions, m^{-1}
l, l', l''	=	distance between heat source and detection point, m
m	=	mass, kg
Q_E	=	electric power, W
q_l	=	heat loss, W
T	=	temperature, K
T_{ac}	=	ac temperature, K
t	=	time, s
u, v	=	indices of summation
w	=	width of sample, m
x, y, z	=	Cartesian coordinates, m
α_s	=	solar absorptance
$\Delta\phi$	=	phase lag, rad
ε_H	=	total hemispherical emittance
θ	=	incident angle, deg
λ	=	wavelength, m
ρ	=	reflectance
σ	=	Stephan–Boltzmann constant, $5.67 \times 10^{-8}\ W\ m^{-2}\ K^{-4}$
ω	=	angular frequency, s^{-1}

Subscripts

GS	=	graphite sheet
H	=	heater
Im	=	imaginary part
L	=	lower
meas	=	measurement
offset	=	offset
Re	=	real part
S	=	sample
Sa	=	absolute
U	=	upper
W	=	wall

Introduction

THE current spacecraft trend toward high density packing of the payload electronics and increased waste heat flux will require the development of lightweight high-thermal-conductivity materials and innovative thermal transport techniques. Aluminum alloys are the most commonly used materials for spacecraft thermal management components because of their high specific thermal conductivity. Several high-thermal-conductivity composite materials, including carbon-carbon composites, metal matrix composites, and polymer matrix composites can replace aluminum alloys for thermal control hardware, resulting in significant mass savings and improvement in performance.[1–3] The high thermal performance of carbon composite materials is attributed to the high thermal conductivity of carbon fibers, which are used as fillers of the composites. The shortcoming of the composite materials is the poor thermal conductivity in the direction normal to the fibers as a result of axial orientation of the carbon fibers. To diffuse heat in composites two-dimensionally, the carbon fibers are laid up in different directions in the plane (e.g. 0, ±45, and 90 deg) and, as a result, effective thermal conductivity in each direction reduces.

Recently, a high-thermal-conductivity graphite sheet has been developed.[4] This graphite sheet ($100 \pm 2\ \mu m$ in thickness and $0.84\ g\ cm^{-3}$ in density) has characteristics of lightweight, anisotropy

Received 4 May 2000; presented as Paper 2000-2510 at the AIAA 34th Thermophysics Conference, Denver, CO, 19–22 June 2000; revision received 8 December 2000; accepted for publication 18 December 2000.

*Graduate Student, School of Integrated Design Engineering, 3-14-1, Hiyoshi. Student Member AIAA.
†Research Assistant, Center for Advanced Spacecraft Technology, 3-1-1, Yoshinodai.
‡Professor, Department of System Design Engineering, 3-14-1, Hiyoshi.

and flexibility like a piece of paper, as well as high thermal conductivity. The graphite sheet (GS) is superior to other composite materials in that the GS has plane orientation while carbon fibers have axial orientation, and so, the GS has the same value of thermal conductivity for any in-plane direction.[5]

The goal of this study is to apply the GS as a material for spacecraft thermal control applications such as radiators, thermal doublers, thermal paths, and heaters. To use the GS as a thermal control material, it is essential to know the thermophysical properties such as thermal conductivity, specific heat, total hemispherical emittance, and solar absorptance. So far, detailed thermophysical properties of the GS have not been reported.

The present paper describes the measurement of temperature dependence of thermal diffusivity, specific heat and total hemispherical emittance, and incident angle dependence of solar absorptance for the GS. The in-plane and out-of-plane thermal diffusivities have been measured over the temperature range from 100 to 350 K using a laser heating ac calorimetric method. The standard method for measuring the out-of-plane thermal diffusivity is the laser flash technique, in which one face of a sample is heated by a laser pulse, while the temperature of the other face is detected thorough its thermal radiation.[6] However, the measurement of the out-of-plane thermal diffusivity of GS using the flash technique could not be performed because the GS is a porous material and the radiation from the inside disturbed the exact measurement. Hence, we have attempted to measure the out-of-plane thermal diffusivity of GS simultaneously with the in-plane thermal diffusivity by improving one of the typical in-plane thermal diffusivity measurement techniques—an ac calorimetric method,[7] though the measured out-of-plane thermal diffusivity by this method has a larger than desired uncertainty. The specific heat of the GS has been measured only preliminarily because 1) it is difficult to measure the specific heat of thin and low-density materials by the conventional measurement techniques and 2) unlike the thermal transport properties, the specific heats of graphite materials are independent of the degree of graphitization.[8] The specific heat has been measured simultaneously with the total hemispherical emittance over the temperature range from 173 to 373 K using a transient calorimetric method. The solar absorptance has been calculated by measuring the spectral hemispherical reflectance over the wavelength range from 0.26 to 2.5 μm using a spectroscopic method in the incident angle range from 5 to 60 deg. Additionally, the thermal conductivity and the specific thermal conductivity, defined as thermal conductivity divided by density, have been calculated and discussed by comparing with other high-thermal-conductivity materials.

Graphite Sheet

The GS used in the present study has been prepared from aromatic polyimide films by heat treatment at 2900–3300 K in an inert atmosphere.[4] The process for making highly oriented graphite sheets from polyimide films is as follows: 1) At temperatures between 700 and 900 K, the thermal decomposition reaction proceeds preferentially on the imide group, and a planar and heterocycle carbon precursor with the nitrogen contained are made. 2) Carbonization occurs by denitrification and dehydrogenation, and aromatic rings are developed above 1300 K. 3) At temperatures above 2900 K, lamination layers have been grown, and highly oriented graphite films are produced.

Figure 1 shows the scanning electron microscope (SEM) photos of 1) the surface and 2) the cross-sectional view of the GS structures. It is remarkable that the GS is organized in different structures between the in-plane and the out-of-plane directions. Examining the cross-sectional view of GS (Fig. 1b), there are large vacancies between the layers sporadically. They cause the difficulty in making the out-of-plane thermal diffusivity measurement.

Theoretical Background and Experimental Apparatus

Thermal Diffusivity

A laser heating ac calorimetric method is used to measure both the in-plane and the out-of-plane thermal diffusivities of GS. In this measurement, a modulated laser beam, which is focused, is irradiated upon the front surface of a sample, and the ac temperature is measured by a fine thermocouple, which is attached to the rear face of the sample. The surface heating is supposed because the optical absorption length of the GS is less than 2.4×10^{-8} m.

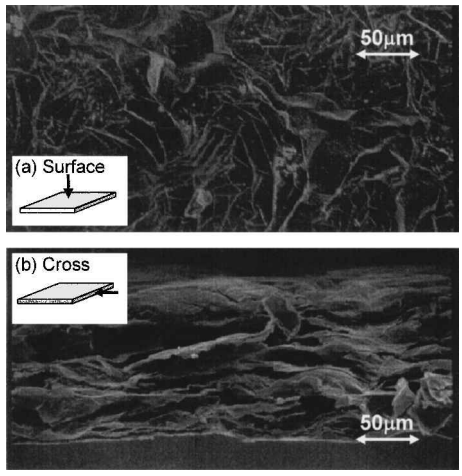

Fig. 1 SEM images of a) surface and b) cross-sectional features of the graphite sheet.

First of all, consider an isotropic medium of the three-dimensional infinite region. Green's function at x at a time t caused by a unit instantaneous heat source at x' at the time t' is

$$G_x(x, t; x', t') = \frac{1}{2\sqrt{\pi a(t - t')}} \left\{ \exp\left[-\frac{(x - x')^2}{4a(t - t')} \right] \right\} \tag{1}$$

Green's functions at y and z can be written in a similar form. The ac temperature response in the medium heated by a modulated point heat source at the point $(0, 0, 0)$ at the rate $\rho c e^{i\omega t}$ from time $t' = -\infty$ to $t' = t$, where ρ is the average density of the media and c is the heat capacity, can be expressed as[9]

$$T_{\text{ac}}(x, y, z, t) = \int_{-\infty}^{t} e^{i\omega t} G_x(x, t; x', t') G_y(y, t; y', t') \times G_z(z, t; z', t')\, \mathrm{d}t' = \frac{1}{4\pi a l(x, y, z)} \times \exp\{-kl(x, y, z) + i[\omega t - kl(x, y, z)]\} \tag{2}$$

where T_{ac} is the ac temperature at the detection point and $\omega = 2\pi f$ is the angular frequency. l can be written as

$$l(x, y, z) = \sqrt{x^2 + y^2 + z^2} \tag{3}$$

k is given by

$$k = \sqrt{\pi f / a} \tag{4}$$

The detected phase lag $\Delta\phi$ of the ac temperature is given by

$$\Delta\phi(x, y, z) = -kl(x, y, z) \tag{5}$$

Combining Eqs. (4) and (5), one has

$$a = \pi f \left[\frac{l(x, y, z)}{\Delta\phi(x, y, z)} \right]^2 \tag{6}$$

From Eq. (6) the in-plane thermal diffusivity for an isotropic material is given as the distance dependence of the phase lag at a fixed frequency. However, in order to obtain both the in-plane and out-of-plane thermal diffusivities simultaneously for high-thermal-conductivity orthotropic materials, the effects of anisotropy and the boundaries of infinite samples need to be considered.[10]

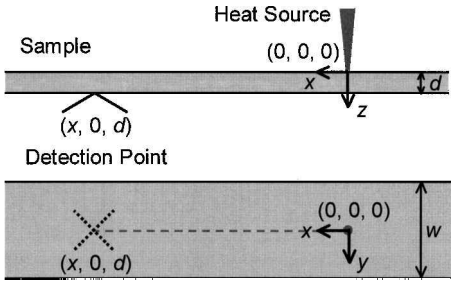

Fig. 2 Sample shape for thermal diffusivity measurement.

In the case of a two-dimensional orthotropic material like GS, which has a different thermal diffusivity in any xy direction (a_{xy}) as compared to the z direction (a_z), the ac temperature response can be written using Green's function as[9]

$$T_{ac}(x, y, z, t) = \frac{\exp[i\omega t - (1+i)k_{xy}l'(x, y, z)]}{4\pi\sqrt{a_{xy}a_z}\,l'(x, y, z)} \tag{7}$$

where

$$l'(x, y, z) = \sqrt{x^2 + y^2 + (a_{xy}/a_z)z^2} \tag{8}$$

$$k_{xy} = \sqrt{\pi f/a_{xy}} \tag{9}$$

In practice, the measurement is performed in the infinite region, and in the case of the high-thermal-conductivity material the periodic thermal energy propagated from the heat source is reflected at the insulated sample edges repeatedly and, as a result, affects the measurement.[10,11] Consider an orthotropic medium with a width w along y axis, a thickness d along the z axis, and a length along the x axis, which is far larger than the thermal diffusion length (which for the GS under consideration is 40 mm in the length while the thermal diffusion length is 7 mm at the most) and can be considered to be an infinite length, as shown in Fig. 2, and there is no heat loss by the conduction to the surroundings. The detected temperature response at $y = 0$, $z = d$ can be described as[10]

$$T_{ac}(x, 0, d, t) = \frac{e^{i\omega t}}{2\pi\sqrt{a_{xy}a_z}}\sum_{v=0}^{\infty}\left\{\frac{\exp[-(1+i)k_{xy}l''(0, v)]}{l''(0, v)}\right.$$

$$\left. + 2\sum_{u=1}^{\infty}\frac{\exp[-(1+i)k_{xy}l''(u, v)]}{l''(u, v)}\right\} \tag{10}$$

where

$$l''(u, v) = \sqrt{x^2 + (uw)^2 + (a_{xy}/a_z)[(2v+1)\,d]^2} \tag{11}$$

The ac temperature T_{ac} can be expressed as

$$T_{ac}(x, y, z, t) = T_{Re}(x, y, z, t) + iT_{Im}(x, y, z, t) \tag{12}$$

where T_{Re} and T_{Im} are the real and the imaginary parts of T_{ac}, respectively. The phase lag is obtained from

$$\Delta\phi(x, y, z, t) = \arctan\left[\frac{T_{Im}(x, y, z, t)}{T_{Re}(x, y, z, t)}\right] \tag{13}$$

For the most precise experiments the measured phase delay $\Delta\phi_{meas}$ contains the constant phase delay $\Delta\phi_{offset}$ caused by the effects of the thermocouple and the experimental equipment, and the measured phase lag can be expressed as

$$\Delta\phi_{meas} = \Delta\phi + \Delta\phi_{offset} \tag{14}$$

The in-plane thermal diffusivity a_{xy}, the out-of-plane thermal diffusivity a_z, and offset value $\Delta\phi_{offset}$ are determined simultaneously by the curve-fitting method, which is based on a simplex algorithm,[12] where the complete phase lag vs distance curve is fitted by Eq. (14).

Table 1 Comparison of measurement results and recommended values

Sample	Recommended value [$\times 10^{-6}$ m^2 s^{-1}]	a_{xy} [$\times 10^{-6}$ m^2 s^{-1}]	a_z [$\times 10^{-6}$ m^2 s^{-1}]
Stainless steel[13]	3.72	3.70	3.32
Pure copper[14]	117	119	56.9

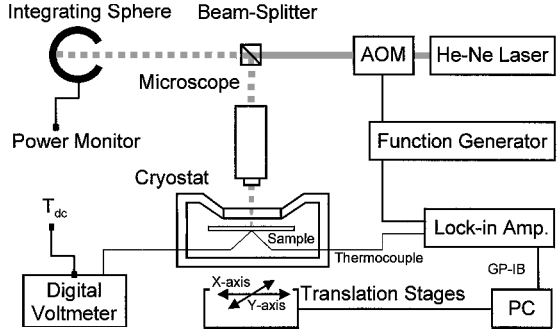

Fig. 3 Schematic diagram of the apparatus for thermal diffusivity measurement.

Figure 3 shows the laser-heating ac calorimetric measurement apparatus,[13] which consists of an ac laser-heating source, a helium (^{4}He) gas continuous flow cryostat to cool a sample, and a measuring system. The measurement is performed under a vacuum condition in order to neglect heat loss by conduction to the surrounding air. The heat source is a He-Ne gas laser whose maximum output power is 10 mW. The intensity modulation of the laser beam at an arbitrary frequency between 1 and 1000 Hz is achieved with an acousto-optic modulator (AOM). The beam diameter is adjusted to less than 10 μm by a microscope. The beam irradiation position is controlled by x–y dual axes translation stages, which are set under the cryostat and can move together with the cryostat. A sample is thermally anchored to a copper cold plate by fixing only both edges of the sample. Temperature in the cryostat is controlled with a heater and ^{4}He gas. Onto the rear face of the sample, a cross junction of a chromel-constantan thermocouple (25 μm in diameter) is attached, and both dc and ac temperatures are simultaneously measured with its two independent terminals. The dc temperature gives a rise of the sample temperature from its background, and the ac temperature gives information of thermal diffusivity in its amplitude and phase delay, detected by means of a lock-in amplifier. The function generator provides the frequency signal of the AOM and the reference frequency of the lock-in amplifier. The data acquisition and the control of laser beam operation are performed using a personal computer.

Reliability of this apparatus and method were confirmed by checking the thermal diffusivities of stainless steel (Standard Reference Material, SRM1461, 0.5 mm in thickness), which were obtained from the National Institute of Standards and Technology, and pure copper (0.1 mm in thickness). A series of four measurements using this apparatus was carried out with stainless-steel material and copper, respectively.[10] Average values of these measurements are listed in Table 1. The measured in-plane thermal diffusivities a_{xy} of stainless steel[13] and pure copper[14] were in good agreement with recommended values within ±3.5 and 1.7%, respectively. The out-of-plane thermal diffusivities a_z of stainless steel and pure copper were systematically underestimated by about 11 and 52%. The out-of-plane thermal diffusivity a_z of a thinner sample with higher thermal diffusivity is measured in larger disagreement with the recommended value. In the case of the GS, because the values of the thickness and the out-of-plane thermal diffusivity are intermediate between stainless-steel and copper samples, the out-of-plane thermal diffusivity a_z should be systematically underestimated by 11–52%. It is true that this uncertainty is very large, but this simultaneous method based on the ac technique will be a better way than any other methods for the GS having large anisotropy and porosity.

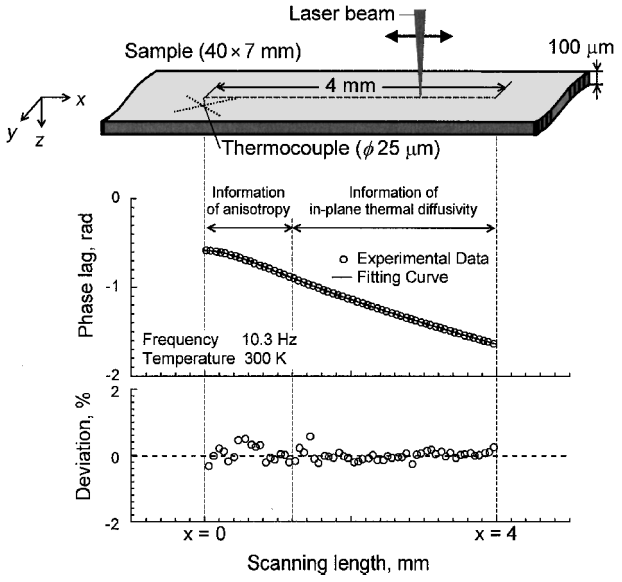

Fig. 4 Sample shape for thermal diffusivity measurement and typical example of measured phase lag vs distance and fitting curve of graphite sheet.

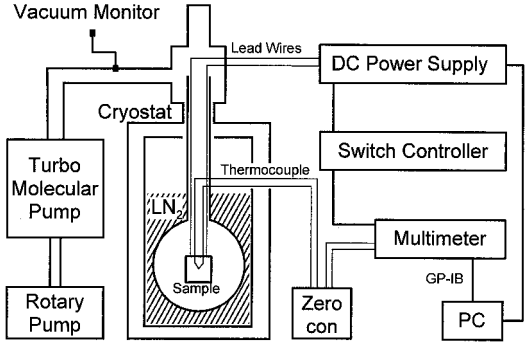

Fig. 5 Schematic diagram of the apparatus for specific heat and total hemispherical emittance measurement.

Figure 4 shows the shape of the GS sample and a typical example of the phase lag vs distance measurement result and fitting curve from Eq. (14). Through the measurement the modulating frequency was adjusted with the selected temperature so that the thermal diffusion length would be in a constant range (3.5–7.0 mm).[10]

Specific Heat and Total Hemispherical Emittance

A transient calorimetric method is used to measure the specific heat and the total hemispherical emittance. A sample with a mass m_S and a surface area A_S is placed in a vacuum spherical vessel that is evacuated to high vacuum and cooled at a temperature T_W. The sample can lose heat only by radiation to the walls of the vessel and by conduction through lead wires. The inner walls of the spherical vessel are essentially black, and electrical heating leads are attached to an internally mounted heater in the sample. The equation of energy balance, when the electric power is changed from Q_E to Q'_E ($Q_E \neq Q'_E$), can be expressed as

$$m_S c_S(T_S)\frac{\mathrm{d}T}{\mathrm{d}t} = Q'_E - \varepsilon_{\mathrm{HS}}(T_S)\sigma A_S\left(T_S^4 - T_W^4\right) - q_l \qquad (15)$$

where $\mathrm{d}T/\mathrm{d}t$ is the rate of change of sample temperature with time. The specific heat and the total hemispherical emittance of the sample are determined simultaneously by a simplex method,[12] where the measured temperature as a function of time is fitted by Eq. (15).

The specific heat and total hemispherical emittance measurement is performed with the apparatus illustrated in Fig. 5 (Ref. 15). The apparatus consists of a sample vessel, a liquid nitrogen (LN_2) cryostat, a measuring system, and a vacuum system. The spherical sample vessel (250 mm in diameter), which is made of copper to obtain a uniform temperature distribution and a stability of temperature throughout the measurement, is located at the bottom of the cryostat. The sample vessel is cooled by LN_2, and the pressure in the sample component is kept at 10^{-5} Pa with a turbomolecular pump. The inner walls of the sample vessel are painted with a black paint (CHEMIGLAZE Z306), which has high total hemispherical absorptance. The data acquisition is performed with a personal computer. The sample is suspended at the center of the vessel by means of lead wires. The sample is made in a "sandwich" form as shown in Fig. 6. Two test materials, 30 mm square, and an electrically insulated sheet heater are accurately bonded using an epoxy adhesive. The temperature of the sample is measured by a chromel-alumel thermocouple (50 μm in diameter), which is attached to the center of the sample. Constantan wires (Cu: 55%, Ni: 45%, 50 μm in diameter) are used to supply electrical power.

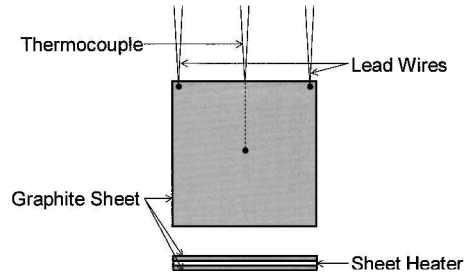

Fig. 6 Sample configuration for the specific heat and total hemispherical emittance measurement.

Provided that the heat capacity of the adhesive is small enough to neglect, the heat capacity of the sample can be described as

$$m_S c_S = m_{\mathrm{GS}} c_{\mathrm{GS}} + m_H c_H \qquad (16)$$

The specific heat of the GS can be obtained from

$$c_{\mathrm{GS}} = (m_S c_S - m_H c_H)/m_{\mathrm{GS}} \qquad (17)$$

To separate the heat capacity of the GS from that of the sheet heater, the measurement is carried out in the following steps: 1) the specific heat and the effective total hemispherical emittance of the sheet heater only (without the GS) are measured; 2) the specific heat and the total hemispherical emittance of the sample composed of the heater and the GS are measured; 3) the specific heat of the GS is calculated from Eq. (17).

Uncertainty of the measurement is attributed to 1) temperature measurement by the thermocouple (±0.77%), 2) current measurement (±0.11%), 3) surface area of the sample measurement (±0.02%), 4) mass measurement (±0.01%), 5) standard deviation between experimental data and fitting curve (±2.78%), 6) temperature gradient within the test sample (less than ±0.001%), 7) heat loss through the lead wires, and 8) heat capacity of the adhesive, which contributes to the specific heat value. The effect of 7), which is less than ±1.0%, was experimentally estimated and calibrated.[12] The specific heat of the adhesive could not be measured, and so we roughly estimated the impact of 8) to be less than 13% using a maximum specific heat of the epoxy resin (<2100 J kg^{-1}K^{-1}), which was obtained from Ref. 16. The combined standard uncertainty of the total hemispherical emittance measurement was estimated to be about ±3.0%, and that of the specific heat measurement was estimated to be less than ±14.5%.

We performed the verification test using pure copper (99.99%). The measured specific heat of the copper sample corresponded to the recommended value within 13.5%, and the total hemispherical emittance corresponded within 2.0% to the emittance measured by a steady calorimetric method with the same measuring system. The reliability of the measured total hemispherical emittance by the steady method with this system was confirmed by comparing with the calculated total hemispherical emittance using the optical constants, which were measured with the Fourier transform infrared

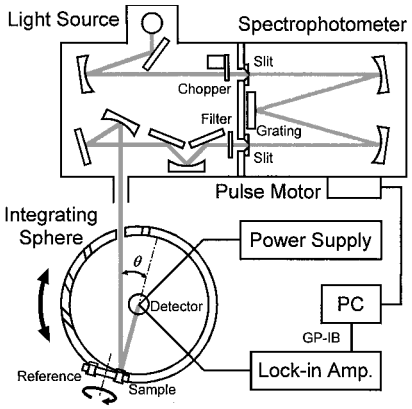

Fig. 7 Schematic diagram of the apparatus for spectral hemispherical reflectance measurement.

spectroscopy in the wavelength range from 2.5 to 100 μm, using aluminum-deposited polyimide films. The measured total hemispherical emittance corresponded to the calculated one within 7.0% (Ref. 17).

Solar Absorptance

The solar absorptance is calculated using the spectral reflectance $\rho_{Sa}(\lambda, \theta)$. Provided that the sample is opaque, the spectral absorptance $\alpha_{Sa}(\lambda, \theta)$ is given as

$$\alpha_{Sa}(\lambda, \theta) = 1 - \rho_{Sa}(\lambda, \theta) \tag{18}$$

The solar absorptance α_S for an incident angle θ is given as

$$\alpha_S(\theta) = \frac{\int_{\lambda_L}^{\lambda_U} \alpha_{Sa}(\lambda, \theta) J(\lambda)\, d\lambda}{\int_{\lambda_L}^{\lambda_U} J(\lambda)\, d\lambda} \tag{19}$$

where $J(\lambda)$ is the spectral distribution of solar radiation, and λ_U, λ_L correspond to the upper and the lower bounds of the wavelength range for the measurement.

Figure 7 shows the spectral reflectance measurement apparatus, which consists of a spectrophotometer, an integrating sphere, and a measuring system.[18] The sample (18 mm in diameter) is attached to the inner surface of the sphere, and the center of the sample is on the equator of the sphere. The test sample can be exchanged into the reference sample with a turret mechanism. The integrating sphere (300 mm in diameter) is allowed to rotate around a vertical axis passing through the center of the sample. Several holes are made on the equator to introduce the monochromatic beam into the sphere. The incident angle to the sample can be adjusted by rotating the sphere leaving the position of the spectrophotometer fixed. The incident angles corresponding to the holes are 0, 5, 10, 20, 30, 40, 50, and 60 deg. The inside of the integrating sphere is spray coated with $BaSO_4$ (Eastman White Reflectance Coating). Detectors, which are photomultipliers for the wavelength region of 0.26–1.20 μm, and PbS for 1.20–2.50 μm, are attached to the center of the sphere. The data acquisition and the calculation of the solar absorptance with the measured spectral reflectance, as well as the control of a pulse motor to drive the wavelength scanning mechanism, are performed using a personal computer. The absolute spectral reflectance of a test sample is determined by the following steps: 1) the intensity of the light reflected at the reference and homogenized by the integrating sphere are measured with the detector in the center of the sphere; 2) the intensity of the light reflected at the test sample and homogenized by the integrating sphere are measured; 3) from the intensity ratio and the absolute spectral reflectance of the reference material, the absolute spectral reflectance of the test sample is determined.

Uncertainty of the measurement is attributed to 1) the value of the spectral reflectance of the reference sample (±1.0%) and 2) energy loss to the introduce hole (±1.0%). The standard uncertainty is estimated to be less than ±2.0%.

The reliability of the measured solar absorptance was confirmed by comparing with the calculated solar absorptance using the optical constants, similar to the process applied to emittance measurement with the FT-IR. The measured solar absorptance corresponded to the calculated one within 5.0% (Ref. 17).

Results and Discussion

Thermal Diffusivity

The results of the in-plane and out-of-plane thermal diffusivities measurement in the temperature range from 100 to 350 K are shown in Fig. 8. It is clear that both the in-plane and out-of-plane thermal diffusivities of the GS have large temperature dependences, and they decrease as the temperature increases. The value of the in-plane thermal diffusivity changes from 3840 to 552×10^{-6} m^2 s^{-1} with the increase of the temperature from 100 to 350 K, and the value of the out-of-plane one changes from 97.2 to 10.7×10^{-6} m^2 s^{-1}. It is confirmed that the GS has extreme anisotropy of thermal diffusivities. The value of the in-plane thermal diffusivity is about 40–50 times larger than that of the out-of-plane result. Additionally, the in-plane thermal diffusivity is very high and far larger than the thermal diffusivities of metals ($<250 \times 10^{-6}$ m^2 s^{-1}).

Specific Heat and Total Hemispherical Emittance

The measured specific heat of the GS, compared with that of other reported data of graphite materials,[8,19–24] in the temperature range from 173 to 373 K is shown in Fig. 9. The specific heat of the GS increases as the temperature increases. The specific heats of graphite materials are, except for extremely low temperatures, almost the same value, independent of the degree of graphitization.[8] Similarly, the specific heat of the GS has the same temperature dependence within 14%.

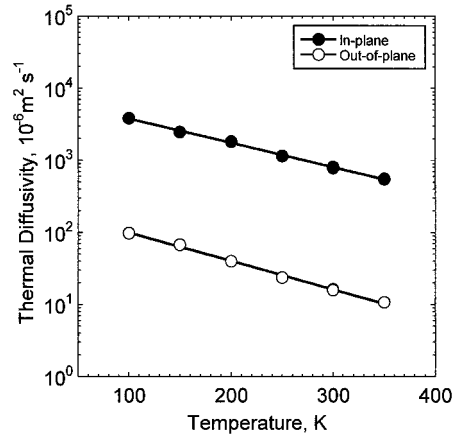

Fig. 8 Temperature dependence of in-plane and out-of-plane thermal diffusivities of graphite sheet.

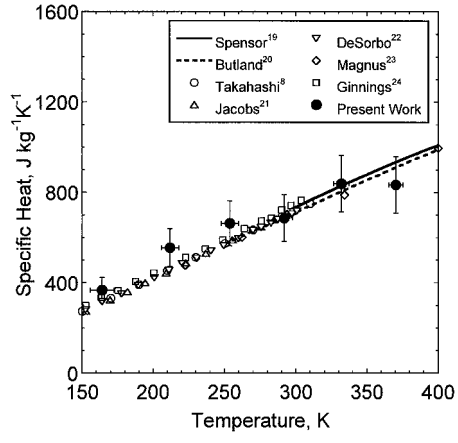

Fig. 9 Temperature dependence of specific heat of graphite sheet, compared with other graphite materials.[8,19–24]

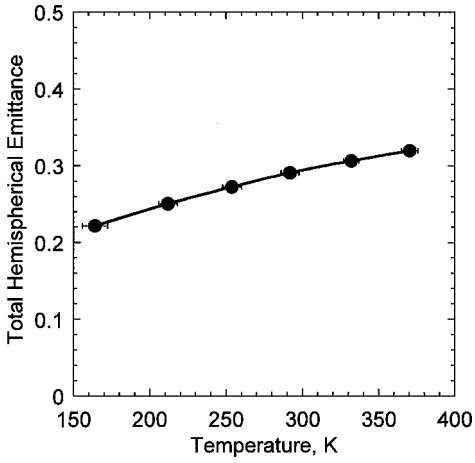

Fig. 10 Temperature dependence of total hemispherical emittance of graphite sheet.

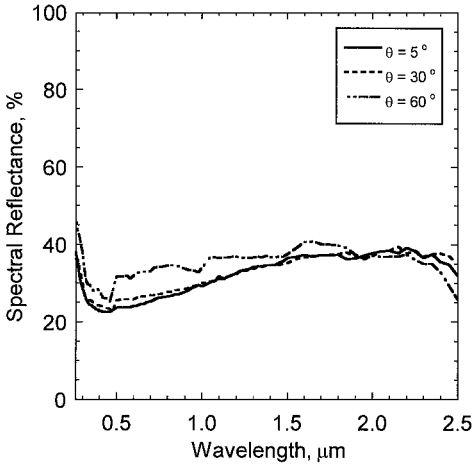

Fig. 11 Spectral hemispherical reflectance of graphite sheet for the incident angles at 5, 30, and 60 deg.

The result of total hemispherical emittance measurement in the temperature range from 173 to 373 K is shown in Fig. 10. The total hemispherical emittance increase as the temperature increases. The value of the total hemispherical emittance changes from 0.22 to 0.32 with the increase of the temperature from 173 to 373 K.

Solar Absorptance

The measured spectral reflectance in the incident angle range from 5 to 60 deg for the GS is shown in Fig. 11. In the ultraviolet region ranging from 0.25 to 0.5 μm, the reflectance decreases steeply with wavelength. In the wavelength region between 0.5–2.2 μm, the reflectance increases with wavelength. Above 2.2 μm the reflectance decreases again. Although the remarkable incident angle dependence of the spectral reflectance between 5 and 30 deg is not confirmed, it is clear that the reflectance at 60 deg is larger than those at 5 and 30 deg. Figure 12 shows the incident angle dependence of the solar absorptance calculated using the measured spectral reflectance of the GS. The values of the solar absorptance for incident angles of 5, 30, and 60 deg are 0.72, 0.72, and 0.67, respectively.

Thermal Conductivity

The thermal conductivity of the GS is calculated using the thermal diffusivity, the specific heat, and the bulk density. The DeSorbo's data[22] (100–250 K) and Butland's equation[20] (250–350 K) for the specific heat are used for calculating thermal conductivity because 1) the measured specific heat of the GS contains larger uncertainty and 2) it was confirmed that the value of the specific heat does not depend on the degree of graphitization.

Table 2 Thermal conductivity, density, and specific thermal conductivity of the GS, pure aluminum, pure copper, pure beryllium, P100 fiber, and K1100 fiber at room temperature

	Thermal conductivity, W m^{-1} K^{-1}	Density, 10^3 kg m^{-3}	Specific thermal conductivity, 10^{-3} W m^2 kg^{-1} K^{-1}
GS			
(in-plane)	466	0.84	554
(out-of-plane)	7.72	0.84	9.19
Pure aluminum[14]	236	2.70	87.4
Pure copper[14]	401	8.96	44.8
Pure beryllium[14]	200	1.85	108
P100 fiber[25] (axis)	293	2.18	134
K1100 fiber[26,27] (axis)	884–917	2.20	402–417

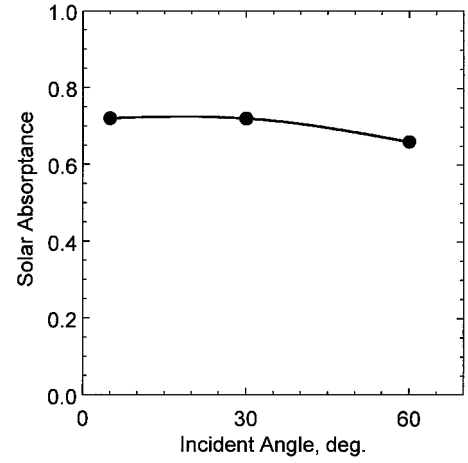

Fig. 12 Incident-angle dependence of solar absorptance for graphite sheet.

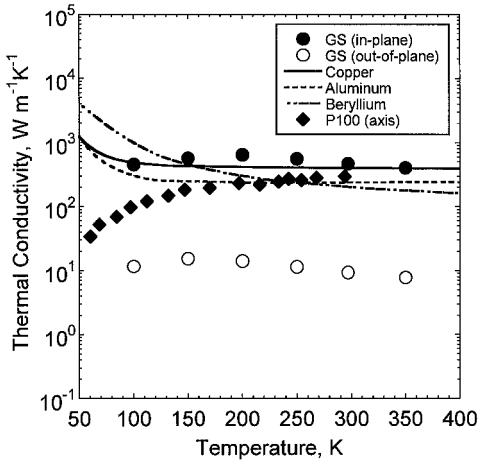

Fig. 13 Temperature dependence of thermal conductivity for graphite sheet, pure metals, and P100 fiber.[14,25]

The calculated thermal conductivity of the GS, compared to the conductivities of pure aluminum, pure copper, pure beryllium,[14] and P100 carbon fiber,[26] are shown in Fig. 13. The in-plane thermal conductivity is significantly greater than those of pure aluminum and pure beryllium and is somewhat larger than the conductivity of pure copper over the present temperature range, whereas the out-of-plane thermal conductivity of the GS is smaller than those of metallic materials. Additionally, the in-plane thermal conductivity for the GS is greater than the conductivity in the axial direction of the P100 fiber.

The specific thermal conductivities, which are calculated by dividing the thermal conductivities of the materials by their densities, of GS, metallic materials, and carbon fibers, are evaluated in Table 2. It is clear that the graphite materials (P100 fiber, K1100, fiber and GS) have far greater specific thermal conductivities than those of metallic materials. Among the graphite materials, the GS is the highest in value of the specific thermal conductivities. Taking into account that the GS can diffuse heat two-dimensionally in the in-plane directions, whereas carbon fibers can diffuse only one-dimensionally, the GS should be a more useful material for spacecraft thermal management components.

Conclusions

To apply a high-thermal-conductivity graphite sheet to a material for spacecraft thermal control applications, thermophysical properties have been measured. The results can be summarized as follows:

1) Temperature dependences of the in-plane and out-of-plane thermal diffusivities were measured simultaneously using a laser heating ac calorimetric method. The large temperature dependence and extreme anisotropy of thermal diffusivities were confirmed.

2) Temperature dependence of the specific heat and the total hemispherical emittance were measured simultaneously using a transient calorimetric method. The specific heat of the GS showed almost the same temperature dependence as the other graphite materials. The total hemispherical emittance increased as the temperature increased.

3) The spectral reflectance was measured using a spectroscopic method, and the incident angle dependence of solar absorptance was calculated.

4) The thermal conductivity and the specific thermal conductivity were calculated.

It was confirmed that this graphite sheet has a high potential as a material for spacecraft thermal control applications on the grounds of its high thermal conductivity and lightweight.

Acknowledgments

We would like to thank H. Kato of the National Research Laboratory of Metrology for much help during this research. We would also like to thank N. Nishiki of the Matsushita Electric Industrial Co., Ltd., for supplying graphite sheets.

References

[1]Juhasz, A. J., and Rovang, R. D., "Composite Heat Pipe Development Status: Development of Lightweight Prototype Carbon-Carbon Heat Pipe with Integral Fins and Metal Foil Liner," NASA TM 106909, May 1995.

[2]Ellis, D. L., "Properties of Graphite Fiber Reinforced Copper Matrix Composites for Space Power Applications," NASA CR 191026, Aug. 1992.

[3]Drolen, B. L., and Johnson, D. S., "High Thermal Conductivity Graphite Composite Thermal Doublers," AIAA Paper 92-0706, Jan. 1992.

[4]Murakami, M., Watanabe, K., and Yoshimura, S., "High-Quality Pyrographite Films," *Applied Physics Letters*, Vol. 48, No. 23, 1986, pp. 1594–1596.

[5]Nagano, H., Kato, H., Ohnishi, A., and Nagasaka, Y., "Measurement of Thermal Diffusivity of Graphite Sheet at Low Temperatures," *High Temperatures-High Pressures* (to be published).

[6]Parker, W. J., Jenkins, R. J., Butler, C. P., and Abbott, G. L., "Flash Method of Determining Thermal Diffusivity, Heat Capacity, and Thermal Conductivity," *Journal of Applied Physics*, Vol. 32, No. 9, 1961, pp. 1679–1684.

[7]Hatta, I., "Thermal Diffusivity Measurement of Thin Films by Means of an AC Calorimetric Method," *Review of Scientific Instruments*, Vol. 56, No. 8, 1985, pp. 1643–1647.

[8]Takahashi, Y., "Glassy Carbon Low-Temperature Thermodynamic Properties," *Journal of Chemical Thermodynamics*, Vol. 2, No. 7, 1970, pp. 847–854.

[9]Carslaw, H. S., and Jaeger, J. C., *Conduction of Heat in Solids*, 2nd ed., Oxford Univ. Press, New York, 1959, pp. 263, 357.

[10]Nagano, H., Kato, H., Ohnishi, A., and Nagasaka, Y., "Measurement of the Thermal Diffusivity of an Anisotropic Graphite Sheet Using a Laser-Heating AC Calorimetric Method," *International Journal of Thermophysics*, Vol. 22, No. 1, 2001, pp. 301–312.

[11]Gu, Y., and Hatta, I., "Effect of Sample Edge in ac Calorimetric Method for Measuring Thermal Diffusivity of Thin Films with High Thermal Diffusivity," *Japanese Journal of Applied Physics*, Vol. 30, No. 5, 1991, pp. 1137, 1138.

[12]Nelder, J. A., and Mead, R., "A Simplex Method for Function Minimization," *Computer Journal*, Vol. 7, No. 4, 1965, pp. 308–313.

[13]Kato, H., "Anisotropic Thermal Diffusivity Measurement Technique by Using Laser-Spot-Heating ac Method," *Proceedings of 20th Japan Symposium on Thermophysical Properties*, Japan Society of Thermophysical Properties, Kanagawa, Japan, 1999, pp. 400–403.

[14]Touloukian, Y. S., Powell, R. W., Ho, C. Y., and Kelemens, P. G., *Thermophysical Properties of Matter*, Vol. 1, Thermal Conductivity of Metallic Solids, IFI/Plenum, New York/Washington, 1970, pp. 9, 24, 81.

[15]Ohnishi, A., Hayashi, T., and Nagano, H., "Measurement of Hemispherical Total Emittance Thermal Control Materials for Spacecraft," *Proceedings of Fourth Japan Symposium on Thermophysical Properties*, Japan Society of Thermophysical Properties, Kanagawa, Japan, 1983, pp. 1–4.

[16]Lynch, C. T., *Handbook of Materials Science*, CRC Press, Boca Raton, FL, 1975, p. 21.

[17]Horikoshi, R., Nagasaka, Y., and Ohnishi, A., "A Method for Calculating Thermal Radiation Properties of Multilayer Films from Optical Constants," *International Journal of Thermophysics*, Vol. 19, No. 2, 1999, pp. 547–555.

[18]Ohnishi, A., and Hayashi, T., "Measurement of Incidence Angle Dependence of Solar Absorptance," *Proceedings of the International Symposium on 'Environmental and Thermal Systems for Space Vehicles*,' European Space Agency SP-200, Dec. 1983, pp. 467–470.

[19]Kelly, B. T., *Physics of Graphite*, Applied Science Publishers, London and New Jersey, 1981, p. 178.

[20]Butland, A. T. D., and Maddison, R. J., "The Specific Heat of Graphite: an Evaluation of Measurements," *Journal of Nuclear Materials*, Vol. 49, No. 1, 1974, pp. 45–56.

[21]Jacobs, C. J., and Parks, G. S., "Some Heat Capacity, Entropy and Free Energy Data for Cyclic Substances," *Journal of American Chemical Society*, Vol. 56, No. 2, 1934, pp. 1513–1517.

[22]DeSorbo, W., and Tyler, W. W., "The Specific Heat of Graphite from 13° to 300° K," *Journal of Chemical Physics*, Vol. 21, No. 10, 1953, pp. 1660–1663.

[23]Magnus, A., "Die Spezifishe Wärme des Kohlenstoffs, Siliziums und Siliziumkarbids bei Hohen Temperaturen," *Annalen der Physik*, Vol. 70, 1923, pp. 303–331.

[24]Ginnings, D. C., and Corruccini, R. J., "Enthalpy, Specific Heat, and Entropy of Aluminum Oxide from 0 to 900," *Journal of Research National Bureau Standards*, Vol. 38, No. 6, 1947, pp. 593–600.

[25]Heremans, J., Rahim, I., and Dresselhaus, M. S., "Thermal Conductivity and Raman Spectra of Carbon Fiber," *Physical Review B,* Vol. 32, No. 10, 1985, pp. 6742–6747.

[26]Adams, P. M., Katzman, H. A., Rellick, G. S., and Stupian, G. W., "Characterization of High Thermal Conductivity Carbon Fibers and a Self-Reinforced Graphite Panel," *Carbon*, Vol. 36, No. 3, 1998, pp. 233–245.

[27]Curran, D. G. T., and Lam, T. T., "Optimal Sizing of Honeycomb Radiators with Embedded Heat Pipes," AIAA Paper 95-2136, June 1995.